Fluorescence Characteristics of Cure Products in Bis(maleimide)/Diallylbisphenol A Resin

John C. Phelan and Chong Sook Paik Sung*

Institute of Materials Science, Polymer Science Program, University of Connecticut, 97 North Eagleville Road, Storrs, Connecticut 06269-3136

Received December 23, 1996; Revised Manuscript Received August 5, 1997[⊗]

ABSTRACT: Curing bis(maleimide) (BMI) with diallylbisphenol A (DABPA) results in the formation of a high-performance thermoset resin. A variety of reactions in which maleimide units are converted to succinimide moieties have been proposed. In order to make spectral assignments for the fluorescence behavior observed during the cure of BMI/DABPA resin and to assess the likelihood that certain types of reactions take place during resin cure, several succinimide model compounds were synthesized from *N*-phenylmaleimide (NPM) and characterized. These model compounds gave fluorescence signals which were red-shifted by 40 nm or more from the emission maximum in DABPA resin, while no fluorescence was observed from the BMI. The BMI was found to quench the fluorescence from DABPA and a Stern−Volmer quenching constant was determined for this pair. Relative fluorescence quantum yields were determined for the model compounds. The DABPA resin component was found to have the highest quantum yield and is likely to be responsible for most of the fluorescence near 356 nm when the resin is excited near 280 nm. A succinimide derivative which arises from a Diels−Alder−Ene reaction sequence was found to have a higher quantum yield than other succinimides which were investigated. This type of structure might be responsible for most of the fluorescence observed in the long wavelength regions. Fluorescence peak shapes and peak positions were found to have a concentration dependence.

Introduction

Bis(maleimide)s (BMI's) have been copolymerized with allyl- or propenyl-substituted aromatic compounds[1−7] as well as with aromatic diamines[8−12] to improve the toughness of BMI-based resins, which are often used in composites. Because the optimization of polymer properties and the production of materials with consistent properties require sensitive analytical methods which can be used to determine the extent of cure, this laboratory has been involved in the application of fluorescence and UV−visible spectroscopy for cure characterization and monitoring.[14−17]

A high-performance thermosetting resin prepared by curing 4,4′ bis-(maleimidodiphenyl)methane (BMI) with 2,2′-bis(3-allyl-4-hydroxyphenyl)propane (DABPA)[1−3] is the resin of interest in this study. The chemical structures of BMI and DABPA are illustrated in Chart 1. Although there have been several reports on the curing of BMI/DABPA resin, a clear mechanism has not yet emerged.[1−6,19−21] This is due to the diverse chemistry of the maleimide group and the difficulty associated with obtaining detailed structural information on thermoset resins. Preliminary studies from our laboratory have indicated that curing BMI/DABPA resin results in complex fluorescence changes.[18] These results, along with other spectroscopic data and their interpretation, will be reported in the following paper. Several reaction types have been implicated in BMI/DABPA resin curing, including Ene, Diels−Alder, homopolymerization, rearomatization, and alternating copolymerization.[1−6,19−21] These processes are summarized in Figure 1. In all of these transformations, maleimide moieties are converted to succinimide groups. This observation prompted us to prepare succinimide derivatives with well-defined structures to help make spectral assignments to explain the fluorescence behavior observed during resin cure. Relative fluorescence quantum yields are determined to assess the contributions of different cure species to the overall fluorescence behavior during cure. To evaluate the spectral changes from dilute solution to the bulk cure state, the concentration dependence of the fluorescence behavior of the model cure products was also studied.

Chart 1. Chemical Structures of Model Compounds

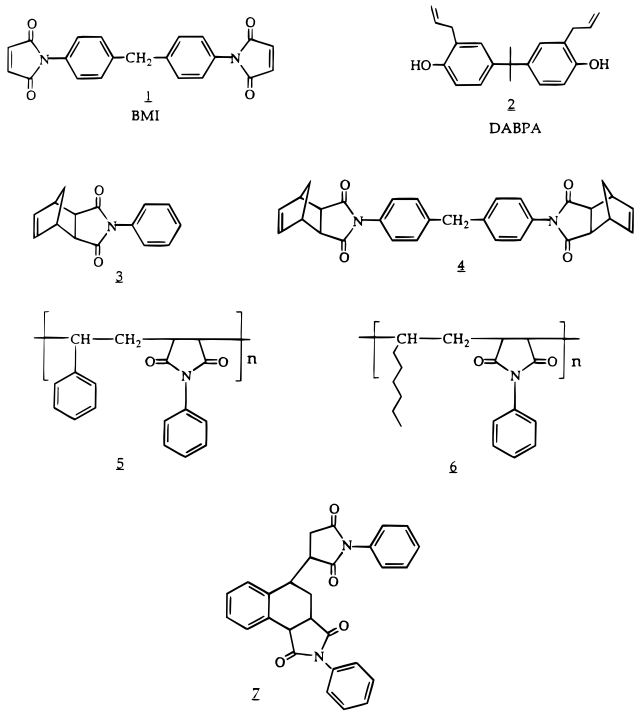

Experimental Section

General Methods and Apparatus. All melting points (mp), glass transition temperatures (T_g), and other thermal transitions were determined on a TA Instrument DSC 2920. The DSC instrument was calibrated with an indium standard. All samples were encapsulated in aluminum pans and heated at 10 °C/

[⊗] Abstract published in *Advance ACS Abstracts,* October 1, 1997.

S0024-9297(96)01888-8 CCC: $14.00

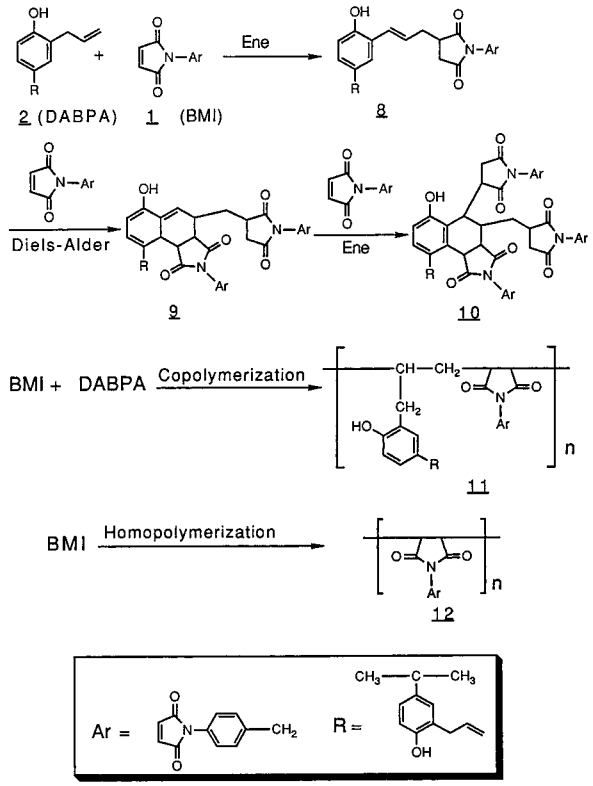

Figure 1. Proposed reaction schemes for BMI/DABPA curing.[1,8,19,21]

min under nitrogen atmosphere. An empty aluminum pan was used as a reference for all DSC measurements. T_g values were taken as the inflection points in the thermograms. Thermogravimetric analysis measurements were made on a TA Instrument high-resolution TGA 2950. Samples were placed in platinum pans and heated at 20 °C/min under nitrogen atmosphere. Infrared spectra were recorded on a Nicolet 60 SX spectrometer. A Perkin-Elmer Lambda 6 UV-Visible spectrometer was used to record UV−visible spectra. A front surfaced mirror from Perkin-Elmer was used as a background in UV-reflection experiments. NMR spectra (^{1}H and ^{13}C) were obtained with a Bruker AC-270 FT-NMR spectrometer. All chemical shifts are reported in ppm (δ) with respect to internal tetramethylsilane. Weight average molecular weights (M_w) and number average molecular weights (M_n) for polymeric and oligomeric materials were determined on a Waters gel permeation chromatograph (GPC). Ultra Styragel columns were used with THF as the eluent at a flow rate of 1 mL/min. Column elution times were calibrated with monodisperse polystyrene standards from Polysciences. Mass spectra (MS) were recorded on a Kratos MS 50 RFA instrument. Elemental analyses were carreied out by Robertson Microlit Laboratories, Inc, Madison, NJ.

Materials. Caution should be exercised when working with any of the chemicals described in this work. For example, *N*-phenylmaleimide is a toxic irritant. BMI and DABPA were provided by Ciba-Geigy. BMI was recrystallized from methanol/chloroform (1:1 vol/vol) before use. Its purity was checked by DSC. The DABPA was used as received. Styrene was washed with 10% aqueous KOH and H_2O, dried over $MgSO_4$, and vacuum distilled before use. Cyclopentadiene was freshly prepared just prior to use by gently heating dicyclopentadiene in a distillation apparatus fitted with a Claisen adapter. The receiving flask was chilled in an ice bath to inhibit the dimerization of cyclopentadiene. Other reagents and solvents were commercially available and used as received. The petroleum ether which was used in this work was low boiling (30−60 °C).

Synthesis of Cure Products. The chemical structures of cure products other than BMI and DABPA are illustrated in Chart 1.

***N*-Phenyl-norbornene-5,6-dicarboximide, 3.**[22a] To 1.76 g (10.2 mmol) of *N*-phenylmaleimide in 3.5 mL of xylene was added 1.01 g (15.3 mmol) of freshly prepared cyclopentadiene. After several minutes, 7 mL of petroleum ether was added to the reaction mixture. A white solid (2.21 g) was filtered from the mixture and then washed with petroleum ether. The product was then recrystallized from xylene and petroleum ether. A second recrystallization from acetone yielded 0.86 g (35%) of white crystals: mp = 142 °C (lit.[22b] 142.5−144.5). TGA, *T* (decomp) = 258 °C. ^{1}H NMR ($CDCl_3$): δ 7.29 (m, 5H), 6.26 (s, 2H), 3.47 (m, 4H), 1.70 (m, 2H). ^{13}C NMR ($CDCl_3$): δ 176.59, 134.41, 131.77, 128.85, 128.34, 126.49, 52.03, 45.59, 45.29. IR (KBr pellet): 2996, 2954, 1705, 1498, 1377, 1184, 740 cm^{-1}. MS (electron impact): *m/e* 239 (M^+) 173, 145, 129, 119, 103, 91, 77, 66, 54, 39, 26. High resolution mass spectrum: calculated for $C_{15}H_{13}NO_2$ (M^+), 239.0946; found, 239.0944. Anal. Calcd for $C_{15}H_{13}NO_2$: C, 75.30; H, 5.48; N, 5.85. Found: C, 74.99; H, 5.56; N, 5.78.

Methylene-4,4′-bis(*N*-phenylbicyclo[2.2.1]hept-2-ene-5,6-dicarboximide), 4. To a slurry of 1.77 g (4.9 mmol) of bis(maleimide) (**1**) in 10 mL of xylene was added 1.09 g of freshly prepared cyclopentadiene. An additional 5 mL of xylene was added, and the mixture was refluxed for 2 min. Petroleum ether was added to the reaction mixture, and an off-white powder (2.38 g) was filtered from the solution. The product was recrystallized from toluene and petroleum ether to yield fine white crystals which were washed with petroleum ether and dried to yield 1.97 g (81%). This material was further purified by recrystallization from chloroform followed by washing with acetone (2 × 10 mL) and petroleum ether (2 × 10 mL) to yield 1.16 g (48%) of a white crystalline material: mp = 261 °C dec; TGA, *T* (decomp) = 270, 510 °C. ^{1}H NMR ($CDCl_3$): δ 7.15 (m, 8H), 6.24 (s, 4H), 3.99 (s, 2H), 3.45 (m, 8H), 1.69 (m, 4H). ^{13}C NMR ($CDCl_3$): δ 176.72, 140.76, 134.52, 129.99, 129.55, 126.58, 52.13, 45.69, 45.42, 41.04. IR (KBr pellet): 2987, 1710, 1514, 1377, 1182, 717 cm^{-1}. MS (electron impact): *m/e* 358, 261, 66, 51, 39. Fast atom bombardment (FAB) mass spectrum: *m/e* 491 (M^+), 309, 186, 155, 135. Anal. Calcd for $C_{31}H_{26}N_2O_4$: C, 75.90; H, 5.34; N, 5.71. Found: C, 75.13; H, 5.32; N, 5.59.

Poly(*N*-phenylmaleimide-*co*-styrene), 5. *N*-Phenylmaleimide (0.92 g, 5.3 mmol) was dissolved in 30 mL of acetone. To the acetone solution was added 0.61 mL of styrene. The reaction mixture was then refluxed for 2 weeks in an air atmosphere. The acetone was distilled and the residue was dissolved in a minimum amount of chloroform. The chloroform solution was poured into 150 mL of stirred methanol. A white solid 1.31 g (97%) was then filtered from the methanol and vacuum dried at room temperature: T_g = 229 °C; *T* (decomp) = 433 °C. ^{1}H NMR ($CDCl_3$): δ 8−6 (broad absorptions, 10H), 4−1 (broad absorptions, 5 H). The proton NMR integrations give a calculated 1:1 copolymer composition. ^{13}C NMR ($CDCl_3$): δ 177.16, 176.28, 131.53, 128.99, 126.43, 55−30 (broad absorptions). IR (film cast on

NaCl): 3100−3000, 3000−2850, 1711, 1499, 1383, 1184 cm^{-1}. GPC: $M_w = 5.9 \times 10^5$; $M_n = 2.6 \times 10^5$. Anal. Found (copolymer): C, 76.79; H, 5.36; N 5.11. This is consitent with a copolymer composition with approximately a 1:1 ratio of styrene and *N*-phenylmaleimide units.

Poly(*N*-phenylmaleimide-*co*-1-octene), 6. To a solution of *N*-phenylmaleimide (4.09 g, 23.6 mmol) in 200 mL of bis(2-methoxyethyl) ether was added 100 mL of 1-octene. The reaction mixture was then refluxed for 22 h, followed by distillation of solvent and excess 1-octene. The concentrated mixture was diluted to 100 mL with methylene chloride, washed with saturated brine and water, and then dried over $MgSO_4$. After the methylene chloride was evaporated, the resulting residue was stirred in methanol and filtered. The resulting solid was dissolved in methylene chloride and then precipitated in methanol, stirred for 24 h, filtered, and dried to yield 3.64 g (54%) of a light yellow solid: T_g = 40 °C; *T* (decomp) = 420 °C. ^{1}H NMR ($CDCl_3$): δ 8−7 (broad absorptions, 50H), 4.5−0.5 (broad absorptions, 213 H). ^{13}C NMR ($CDCl_3$) δ 178 (broad signals, three main peaks), 131.84, 129.04, 128.50, 126.38, 55−35 (broad), 31.72, 29.31, 27.40, 22.57, 14.01. IR (film cast on NaCl): 2954, 2927, 2856, 1709, 1500, 1456, 1381, 1180, 752 cm^{-1}. GPC: M_w = 2270; M_n = 460. The proton NMR integrations indicate that there are approximately 100 octene units for every 83 units of *N*-phenylmaleimide. Anal. Found: C, 75.66; H, 8.80; N, 4.24. On the basis of the nitrogen content, this corresponds to a copolymer composition with approximately 100 octene units for every 74 units of *N*-phenylmaleimide.

2-Phenyl-5-(phenyl-2,5-dioxopyrolidin-3-yl)-3a,-4,5,9b-tetrahydrobenzoisoindole-1,3-dione, 7. To a mixture of *N*-phenylmaleimide (0.81 g 4.7 mmol) in toluene was added styrene (0.25 mL). After 24 h of stirring at 35 °C, there appeared to be no appreciable reaction by TLC. At this point, 0.152 g of aluminum chloride, as a catalyst, was added, and the reaction mixture was allowed to stir for an additional 16 h. The reaction mixture was poured over ice and then extracted with 200 mL of methylene chloride or chloroform. The aqueous layer was separated, and the methylene chloride layer was washed with 10% sodium carbonate (2 × 50 mL) and water (2 × 50 mL), dried over $MgSO_4$, and evaporated to yield a light yellow solid which was recrystallized from toluene. The crystals were washed with petroleum ether and dried in a vacuum oven at 50 °C to yield 0.30 g (28%) of compound **7**. Differential scanning calorimetry of this material showed multiple melting transitions {140, 170, 183 (max), 198 °C}. When cooled and reheated, this material shows a glasslike transition near 106 °C. It should be noted that when compound **7** is heated for 1.5 h at 200 °C, no sign of decomposition is observed by proton NMR. Decomposition temperature by TGA: *T* (decomp) = 417 °C. Spectral data for compound **7** are as follows: ^{1}H NMR ($CDCl_3$): δ 7.91 (d, J = 7.7 Hz, 1H), 7.15 (d, J = 7.7 Hz, 1H), 7.38 (m, 12 H), 4.22 (d, J = 8.8 Hz, 1H), 3.81 (m, 1H), 3.43 (m, 2 H), 2.93 (m, 1H), 2.51 (m, 2H), 2.22 (m, 1H). ^{13}C NMR ($CDCl_3$): δ 177.52, 177.40, 175.00, 174.57, 134.78, 131.67, 130.88, 129.50, 129.20, 129.12, 128.78, 128.71, 128.12, 127.98, 127.64, 126.32, 44.47, 42.35, 37.91, 37.05, 31.88, 29.63. IR (KBr pellet): 3068, 2924, 1710, 1498, 1383, 1179, 750, 694 cm^{-1}. MS (electron impact): *m/e* 450 (M^+), 275, 175, 155, 129, 91, 69, 57, 43, 29; High-resolution mass spectrum: calculated for $C_{28}H_{22}N_2O_4$ (M^+), 450.1580; found, 450.1577. Anal. Calcd for $C_{28}H_{22}N_2O_4$: C, 74.65; H, 4.92; N, 6.22. Found: C, 74.85; H, 5.16; N, 5.93.

Reaction of *N*-Phenylmaleimide with Styrene (No Catalyst). To a solution of 0.90 g of *N*-phenylmaleimide in 50 mL of toluene was added 0.6 mL of styrene. After several days of refluxing, the reaction mixture was allowed to evaporate. The resulting yellow solid was stirred in petroleum ether, filtered, washed with petroleum ether, and dried to yield 1.09 g of product. ^{1}H NMR analysis showed this material to be a mixture of compound **7**, copolymer **5**, and *N*-phenylmaleimide. The reaction mixture was stirred in 75 mL of methanol to remove *N*-phenylmaleimide from methanol-insoluble products **5** and **7**. A mixture of **5** and **7** (0.67 g) was separated by column chromatography {silica gel, 63 μm mesh, eluted first with ethyl acetate and then with chloroform}. The ethyl acetate fractions which only showed compound **7** by thin layer chromatography, were combined and evaporated to yield 0.31 g of adduct **7**, which was further purified by recrystallization from toluene. The fractions of chloroform were combined and evaporated to yield 0.13 g of a light yellow film. The film was dissolved in a minimum amount of chloroform, precipitated into 60 mL of methanol, filtered, and dried to yield 0.11 g of copolymer **5**. The identities of products **5** and **7** obtained in this preparation were confirmed by comparison of their ^{1}H NMR and FT-IR spectra with those of previously characterized samples of these materials.

Results and Discussion

1. Model Succinimides. The model compounds investigated in this work are shown in Chart 1. The starting materials bis(maleimide) (BMI) and diallylbisphenol A (DABPA) are labeled **1** and **2** respectively. Adducts **3** and **4** were of interest because the phenylsuccinimide rings are fused to carbocycles in which the only aromatic rings are those from phenylsuccinimide moieties. This feature allowed us to examine the fluorescence characteristics of a phenylsuccinimide unit without interference or contributions from neighboring aromatic groups. Adduct **7** was of interest because this type of structure is believed to form during BMI/DABPA curing.[8] In a mechanism suggested by Stenzenberger,[8] DABPA is converted to a styrene-like intermediate after an initial Ene reaction with a maleimide unit of BMI as shown in the top part of Figure 1. The styrene-like intermediate is believed to undergo a Diels−Alder reaction with a maleimide group and finally re-aromatize with the aide of a phenylmaleimide group to yield a structure (**10**) which is similar to model compound **7**,[8] as illustrated in the second part of Figure 1. A mechanism in which the rearomatization step does not involve a phenylmaleimide unit has been proposed by King et al.[1] To assess the likelihood of these scenarios, styrene (**8**) was allowed to react with *N*-phenylmaleimide (**9**) in refluxing toluene as shown in Figure 2. In addition to obtaining **7**, an alternating copolymer (**5**) was obtained. This possibility is indicated in the third part of the Figure 1. This result suggests that the structure arising from a Diels−Alder−Ene reaction sequence as well as from alternating copolymerization might be formed during BMI/DABPA curing. Hall et al. observed similar behavior in the reaction of a substituted maleic anhydride with styrene.[23a] These

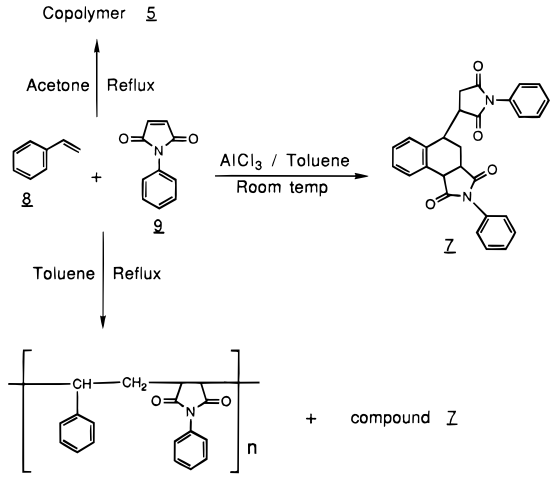

Figure 2. Reactions of styrene with *N*-phenylmaleimide.

authors found that (carbomethoxy)maleic anhydride reacts with styrene to yield a 1:1 copolymer, a Diels–Alder–Ene adduct, and an adduct formed by two consecutive Diels–Alder reactions (Wagner–Jaureg adduct).[23] Adjustment of reaction conditions allowed us to obtain adduct **7** or copolymer **5** as the main product. Styrene reacts with *N*-phenylmaleimide in toluene in the presence of aluminum chloride at room temperature to yield adduct **7**. No copolymer was detected under these conditions. When *N*-phenylmaleimide and styrene were allowed to react in refluxing acetone (no catalyst) only copolymer **5** was obtained. These results are illustrated in Figure 2. The alternating structure of copolymer **5** might be due to charge transfer interactions between *N*-phenylmaleimide and styrene during the assembly of the polymer chain. Evidence of charge transfer complexes during the copolymerization of styrene and with *N*-phenylmaleimide has been reported.[24] There have been several reports on charge transfer copolymerizations involving *N*-phenylmaleimide. This compound has been shown to undergo alternating copolymerizations with styrene, vinyl acetate, and MMA in benzene solution.[24]

An oligomeric material **6** consisting of of *N*-phenylmaleimide and 1-octene units was obtained by refluxing these materials in bis(2-methoxyethyl) ether. Proton NMR analysis indicated that the *N*-phenylmaleimide and 1-octene units were incorporated in approximately an 83:100 ratio. This material was of interest because it permitted for the evaluation of the influence of a short chain structure on the fluorescence characteristics of a phenylsuccinimide group. The styrene/*N*-phenylmaleimide copolymer was used to examine the effect of a neighboring aromatic ring and polymeric backbone on the fluorescence of phenylsuccinimide moieties.

2. Fluorescence Studies of Model Compounds in THF Solution. As previously mentioned, BMI/DABPA resin undergoes complex fluorescence changes upon curing. Therefore, the fluorescence characteristics of compounds **1**–**7** were of interest. No appreciable fluorescence signals are detected for BMI (**1**) (either in solution or the solid state). The fluorescence excitation and emission spectra of the remaining model compounds in THF solution are shown in Figure 3. As can be seen in Figure 3, DABPA (spectrum A) has an excitation maximum near 280 nm and an emission maximum near 304 nm. The excitation peak near 280 nm is due to the characteristic phenolic structure[30a] because the UV–vis spectrum of DABPA displays an absorption band

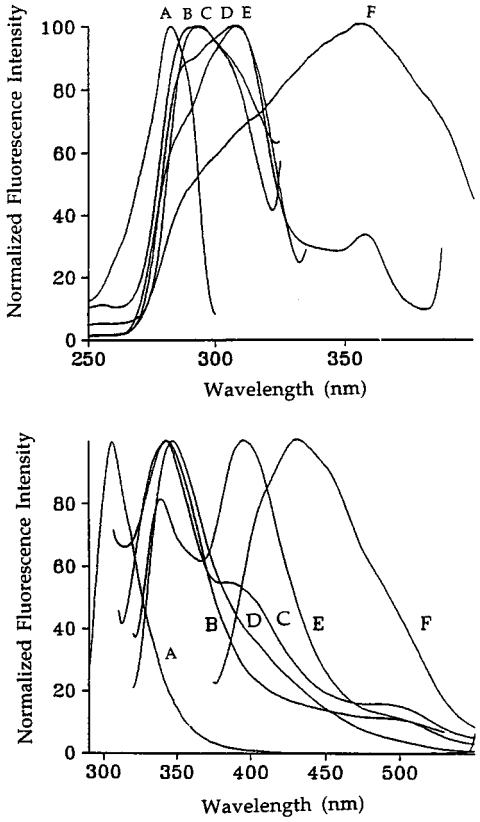

Figure 3. Fluorescence excitation spectra (top) and emission spectra (bottom) of model compounds in THF: (A) compound **2**, 3.24×10^{-6} M; (B) copolymer 5, 6 mg/mL; (C) compound **7**, 4 mg/mL; (D) compound **4**, 3.5 mg/mL; (E) compound **3**, 7 mg/mL; (F) oligomer **6**, 5.4 mg/mL. Excitation and emission spectra are scanned at the maximum emission or excitation wavelengths respectively.

near 280 nm. It should be noted that a neat sample of DABPA displays a fluorescence excitation peak near 280 nm and an emission peak near 350 nm. The differences in fluorescence emission of DABPA in THF and a neat state might be due to polarity differences. It is well-known that fluorescence emission is often sensitive to solvent polarity.[30b]

A THF solution of model compound **3** (spectrum E) shows a fluorescence excitation peak centered at 307 nm and an emission peaks centered at 340, 400 (maximum), and 500 nm as shown in Figure 3. It should be noted that *N*-phenylmaleimide does not fluoresce. Therefore, the conversion of maleimide units to succinimide moieties during the curing of BMI/DABPA resin is expected to give rise to fluorescence signals associated with phenylsuccinimide rings.

Figure 3 shows that model compound **4** (spectrum D) has a fluorescence excitation peak centered at 295 nm and emission peaks at 340 (maximum), 394, and 500 nm. According to mechanisms in Figure 1, a carbocyclic structure is added to BMI units during the curing of BMI/DABPA resin. Therefore, compounds **3** and **4** serve to model the effects of adding carbocyclic structure to phenylmaleimide units. Although compounds **3** and **4** have identical chromophores, there are differences in their fluorescence characteristics. Both compounds have emission peaks near 340, 400, and 500 nm. However, the relative intensities of the 340 and 400 nm peaks are different for these two substances. The fluorescence from these compounds seems to be associated with phenylsuccinimide moieties since these structures do not contain any other types of aromatic rings.

Because structure **7** strongly resembles "final" cure species (structure **10**, Figure 1) for BMI/DABPA curing, its fluorescence properties are of great interest. As can be seen from Figure 3, model compound **7** (spectrum C) displays a fluorescence excitation peak maximum near 307 nm and an emission peak maximum near 346 nm. In addition, its emission spectrum shows tailing that extends beyond 450 nm.

Copolymer **5** was used to examine the effect of a neighboring aromatic ring and a polymeric backbone on the fluorescence of a phenylsuccinimide moiety. This copolymer (spectrum B) shows a fluorescence excitation peak maximum near 290 nm and an emission maximum near 343 nm as shown in Figure 3. The fluorescence emission spectrum of this substance also shows tailing that extends beyond 450 nm. The fluorescence characteristics of this polymer are most similar to those of adduct **7**.

Structure **6** (spectrum F) shows a fluorescence excitation peak near 360 nm and an emission peak near 435 nm in THF solution as shown in Figure 3. Structure **6** permits the examination of the influence of an oligomeric environment on the fluorescence associated with a phenylsuccinimide ring without interference or contributions from other aromatic groups. The differences in the fluorescence characteristics of copolymer **5** and **6** can be understood as follows: The fluorescence emission of **5** can be thought of as a composite of fluorescence spectra from a phenyl ring (short wavelength contribution) and a phenylsuccinimide ring (longer wavelength contribution). Therefore, a larger contribution to fluorescence from the phenyl ring would cause the emission maximum in **5** to occur at a shorter wavelength than that of **6**.

The imide model compounds do not show distinct peaks in their UV−visible absorption spectra corresponding to their fluorescence excitation maxima. However, these compounds do show tailing in the 280−400 nm range if their concentration is sufficiently high. Broad, long wavelength absorption (greater than 330 nm) in polyimides has been assigned to charge transfer interactions by several researchers.[25−28] Absorption in this region has been assigned to a $\pi-\pi^*$ transition due to a shift of electron density from the aromatic substituent to the imide unit.[25−28] The fluorescence emission spectra of the imide model compounds in this work all show fairly broad emission peaks and tailing. Characteristics such as these have also been attributed to charge transfer interactions in polyimides.[29]

Comparison of the fluorescence emission spectra in Figure 3 shows that the emission maxima of the succinimide derivatives are typically red-shifted by 40 nm or more from the emission maximum in DABPA. In the case of oligomeric imide, **6**, fluorescence emission is nearly 130 nm red-shifted from DABPA emission. Therefore, during the curing of BMI/DABPA, one would expect to observe emissions associated with phenylsuccinimide rings to occur at longer wavelengths than those associated with phenolic structures. Any overlap between phenylsuccinimide and phenolic emission should be small. In addition, the relative quantum yield (Φ_f) of DABPA is 7−25 times greater than those of the phenylsuccinimide derivatives. This observation further suggests that short wavelength emissions will be almost exclusively due to phenolic structure. The relative quantum yields of the model compounds and DABPA are listed in Table 1. These were obtained by comparing the ratio of fluorescence emission intensity to UV absorbance at the excitation wavelength used for the sample with that of 9,10-diphenylanthracene (DPA) standard, as illustrated in eq 1. Comparisons of the

Table 1. Relative Fluorescence Quantum Yields of Model Compounds in THF Solution Measured at Emission Maxima

compound	relative quantum yields
1	nonfluorescent
2	25.19
3	1.00
4	2.41
5	2.42
6	2.38
7	3.78

$$\frac{\Phi_{\text{sample}}}{\Phi_{\text{DPA}}} = \frac{I_{\text{f sample}}/A_{\text{sample}}}{I_{\text{f DPA}}/A_{\text{DPA}}} \quad (1)$$

relative quantum yields and emission peak maxima reveal that fluorescence signals from the phenolic structures can be monitored in a "short" wavelength region while fluorescence associated with phenylsuccinimide units can be monitored in a longer wavelength region during BMI/DABPA resin curing.

3. Simulation of Physical Changes during Resin Cure. Although "small" molecules with well-defined structures are useful models for polymers, one needs to keep in mind that there are fundamental differences between polymers and small molecules. In a polymeric system, chromophores often occur regularly within the main chain or as pendent groups. As a result, the local concentrations of chromophores are high, both in dilute solution or in the solid state. Therefore, complex formation is more probable in polymers than in dilute solutions of small molecules. Complex formation in polymers can often be observed by fluorescence spectroscopy.[29,32] In addition, solid state fluorescence measurements which are made on polymeric or nonpolymeric materials may be different than those made in dilute solution. In the solid state, functional groups are situated much closer to each other than in dilute solution which means that excimer formation and/or charge-transfer interactions are more likely.[29,32,33] To understand curing processes thoroughly, consideration should be given to the chemical change, as well as the physical changes, which accompany curing. As materials are cured, functional groups are transformed, polarity changes, and molecular weight (and viscosity) increases. Upon curing, many polymerization systems pass from a liquid state to a solid state. Fluorescence is known to be sensitive to all of these factors. One can model some of the physical changes which occur during curing by recording fluorescence spectra of model species at increasing concentrations and, finally, in the solid state. With this consideration in mind, the fluorescence characteristics of selected model imides were investigated in both dilute and concentrated solutions. These results are discussed below.

a. Effect of Concentration on Phenylsuccinimide Fluorescence. The fluorescence peak positions and shapes have been found to be concentration dependent for the succinimide derivatives used in this work. The broad tailing observed in the fluorescence emission spectrum of model compound **7** is indicative of a charge-transfer interaction in the excited state. Figure 4 shows fluorescence excitation spectra of **7** at two different concentrations. The excitation peak maximum of the most concentrated solution of **7** is ap-

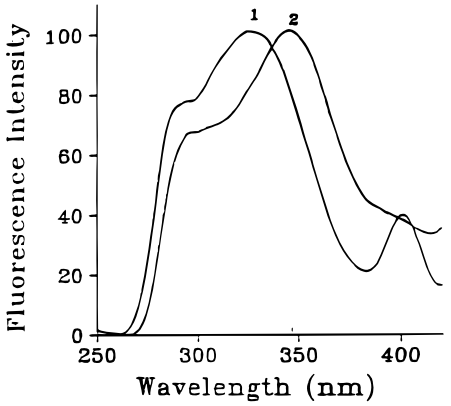

Figure 4. Normalized fluorescence excitation spectra (emission at 456 nm) of compound **7** in THF solution: (1) dilute solution (3 mg/mL); (2) concentrated solution (26 mg/mL).

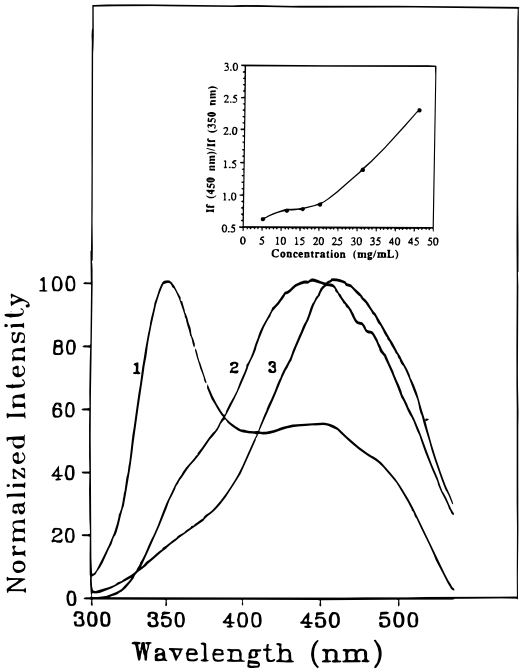

Figure 5. Normalized fluorescence emission spectra (excitation at 280 nm) of oligomer **6** in THF solution: (1) dilute solution (5 mg/mL); (2) concentrated solution (46 mg/mL); (3) neat. The insert shows a plot of fluorescence emission intensity ratio I_f(450 nm)/I_f (350 nm) as a function of concentration for oligomer **6** being excited at 280 nm in THF.

proximately 20 nm red-shifted relative to the less concentrated solution. It should be noted that UV spectrum of 10^{-5} M **7** in THF solution does not display a tail at wavelengths greater than 280 nm. However, a 9×10^{-3} M THF solution of **7** displays a UV absorption tail which extends to about 370 nm. These findings are consistent with the formation of a intermolecular ground state charge-transfer complexes.[29] A more detailed analysis on the effects of concentration on the fluorescence characteristics of phenylsuccinimide groups was carried out on structures **5** and **6**.

b. Effect of Concentration on the Fluorescence of Oligomer 6. Concentration has a direct impact on the fluorescence excitation and emission spectra of structure **6**. Figure 5 shows the fluorescence emission spectra of dilute, concentrated and neat samples of oligomer **6**, when excited at 280 nm. As can be seen, the most dilute sample of **6** has distinct emission peaks at 350 and 450 nm when it is excited at 280 nm. Spectrum 2 in Figure 5 shows that, as concentration is

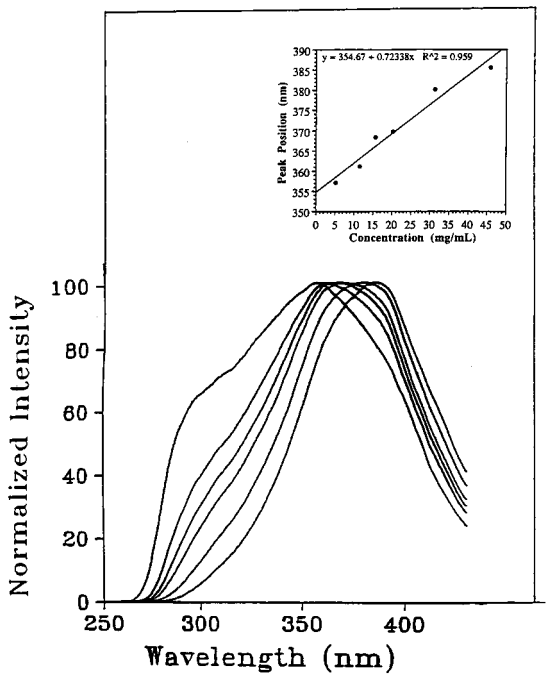

Figure 6. Normalized fluorescence excitation spectra of oligomer **6** in THF solution as a function of concentration: concentration from left to right (5, 12, 16, 20, 31, and 46 mg/mL), with emission at 456 nm. The insert shows a correlation of fluorescence excitation peak maxima of oligomer **6** in THF with concentration (emission at 456 nm).

increased, the ratio of 450 nm peak relative to the 350 nm peak increases to a point where the 350 nm peak becomes a shoulder. Spectrum 3 in Figure 5 corresponds to a neat sample of **6**. This spectrum shows tailing near 350 nm and a large emission peak centered at 460 nm. It should be noted that excitation of structure **6** at 380 nm also results in emission near 450 nm as illustrated in curve F in the lower half of Figure 3. If the peak near 350 nm is associated with uncomplexed polymer and the peak near 450 nm corresponds to complexed material, then a plot of the ratio of relative peak intensities at 450 and 350 nm, I_f(450 nm)/I_f(350 nm), should increase with increasing concentration. The insert shown in Figure 5 shows that this is, indeed, the case.

As previously noted, the fluorescence excitation spectral characteristics of oligomer **6** are concentration dependent. Normalized fluorescence excitation spectra of **6** as a function of concentration are shown in Figure 6. It is clear that as concentration is increased, red-shifting occurs as well as changes in relative peak heights. The most dilute sample of **6** shows a shoulder near 280 nm and a peak maximum near 350 nm. Comparison of this spectrum with spectra of more concentrated solutions shows that as concentration is increased, the intensity of the shoulder near 280 nm is drastically reduced relative to the peak maximum. In addition, the peak maximum shifts from 350 to 380 nm. It is interesting to note that the neat sample of oligomer **6** has two strong peaks: one at 350 nm and another at 380 nm (maximum). A weaker peak occurs near 280 nm. These results are consistent with complexation becoming more favorable at higher concentrations. Just as in the case of fluorescence emission peaks, the fluorescence excitation peaks red-shift as concentration is increased. Concentration can be correlated with excitation peak maxima as shown in the insert of Figure 6.

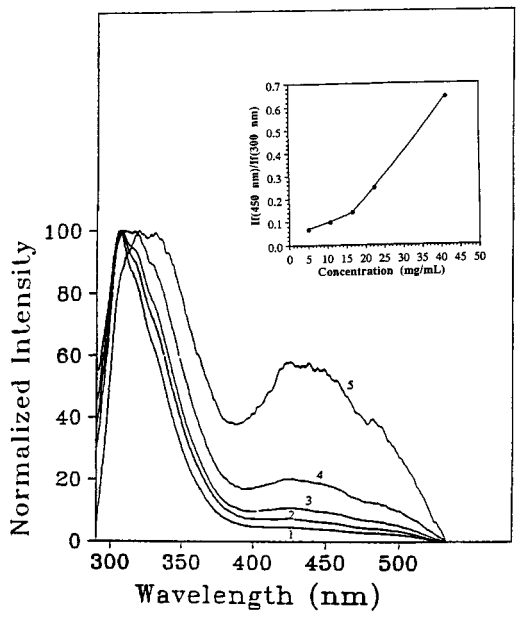

Figure 7. Normalized fluorescence emission spectra (excitation at 280 nm) of copolymer **5** in THF solution as a function of concentration: (1) 5 mg/mL; (2) 11 mg/mL; (3) 17 mg/mL; (4) 22 mg/mL; (5) 41 mg/mL. The insert shows a plot of fluorescence emission intensity ratio I_f(450 nm)/I_f(300 nm) as a function of concentration in THF for copolymer **5** (excitation at 280 nm).

c. Effect of Concentration on the Fluorescence of Copolymer 5. The fluorescence characteristics of styrene/*N*-phenylmaleimide copolymer **5** are concentration dependent. Excitation of copolymer **5** at 280 nm results in emission peaks near 300 and 450 nm. Figure 7 shows normalized fluorescence emission spectra of **5** as a function of concentration. As concentration increases, the peaks near 300 and 450 nm are red-shifted and the intensity of the peak near 450 nm increases relative to the one near 300 nm. Red-shifting of the peak near 450 nm can also be observed by exciting samples of increasing concentration at 380 nm. When samples of increasing concentration of **5** are excited at 280 nm, the ratio of I_f(450 nm)/I_f(300 nm) increases as shown in the insert of Figure 7. This result suggests that the peak near 300 nm is from uncomplexed polymer while the peak near 450 nm is from complexed material.

Figure 8 illustrates that the excitation spectrum of copolymer **5** is red-shifted as concentration is increased. The red-shifting in the excitation spectrum with increasing concentration suggests that ground state intermolecular charge transfer complexation may be occurring. Concentration can be correlated with excitation peak maxima as shown in the insert of Figure 8. Viallat et al. observed similar charge-transfer behavior for solutions of *N*-phenylphthalimide and poly(ether imide).[29] They reported that *N*-phenylphthalimide has a fluorescence peak centered at 350 nm which progressively red-shifts to 395 nm as concentration is increased. In the case of poly(ether imide), Viallat et al. observed two peaks in the excitation spectrum. As they increased the poly(ether imide) concentration, the ratio of the longer wavelength peak relative to the shorter wavelength peak also increased.[29]

d. Fluorescence Quenching. As previously mentioned, BMI is nonfluorescent, while DABPA is highly fluorescent. However, a 1:1 molar mixture of BMI and DABPA (prepared by melting BMI in DABPA) is nonfluorescent. Furthermore, the fluorescence intensity of

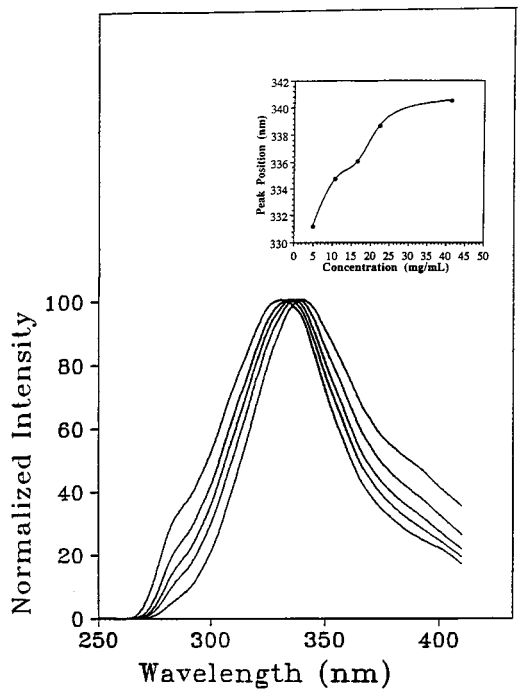

Figure 8. Normalized fluorescence excitation spectra (emission 456 nm) of copolymer **5** in THF solution as a function of concentration. Concentration increases from left to right (5, 11, 17, 22 , and 41 mg/mL). The insert shows a correlation of fluorescence excitation peak maxima of copolymer **5** with concentration in THF (emission at 456 nm).

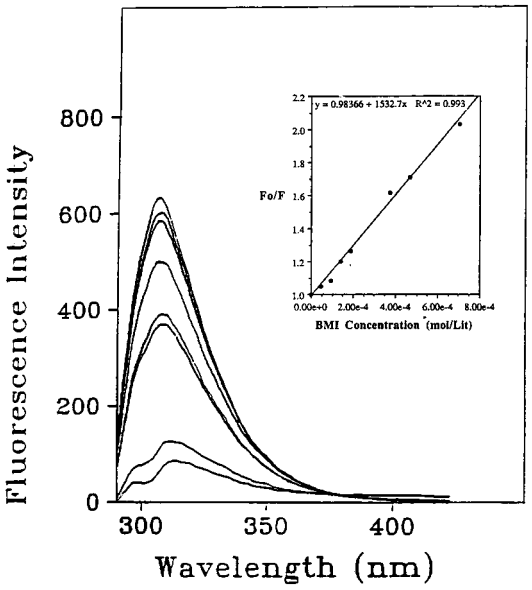

Figure 9. Fluorescence emission spectra of DABPA (3.24×10^{-6} M) in THF in the presence of increasing amounts of BMI (excitation at 280 nm). Concentration of BMI increases from top to bottom (0, 4.676×10^{-5}. 9.352×10^{-5}, 1.403×10^{-4}, 3.741×10^{-4}, 4.676×10^{-4}, 7.014×10^{-4} mol/L). The insert shows a Stern−Volmer plot for BMI quenching of DABPA in THF.

DABPA in solution is reduced by the presence of BMI. Figure 9 shows that DABPA fluorescence intensity decreases as BMI concentration is increased, thereby implicating BMI in the fluorescence quenching process. Some events which lead to quenching are: energy transfer, complex formation, and collisional encounters. Collisional quenching of fluorescence can be described by the Stern−Volmer equation,[30] as shown in eq 2. In the Stern−Volmer equation, F_o is the fluorescence

$$F_o/F = 1 + k_q\tau_o[Q] = 1 + K_D[Q] \quad (2)$$

intensity in the absence of quencher and F is the fluorescence intensity in the presence of quencher. The terms k_q, τ_o, and K_D represent the bimolecular quenching constant, the fluorophore lifetime in the absence of quencher, and the Stern−Volmer quenching constant respectively. The insert in Figure 9 shows a Stern−Volmer plot for the quenching of DABPA fluorescence by BMI. As can be seen, this plot is linear and has an intercept of 1 as predicted by the Stern−Volmer equation. Therefore, it is likely that the fluorescence quenching of DABPA by BMI is collisional. The slope of the line in Figure 9 yields a value of 1533 liter/mole for a Stern−Volmer quenching constant. Olefins have been known to cause fluorescence quenching,[31] and it is believed that the maleimide C═C double bond is linked to the fluorescence quenching of DABPA. Ware et al. found that dimethoxydiphenyl ethylene quenches the fluorescence of 9,9-dicyanoanthracene in benzene solution.[31] The Stern−Volmer quenching constant for this system is six times less than that for the BMI/DABPA pair. The reason that BMI is a more efficient quencher might be due to a strong association of BMI with DABPA. The DABPA is electron rich whereas the maleimide C═C double bond in BMI is electron deficient due to the electron-withdrawing effects of the imide carbonyl groups. This conclusion is reasonable because quenching efficiency has been observed to have a strong dependency on donor−acceptor properties.[31]

Summary

The synthesis and fluorescence characteristics of several model imides related to BMI/DABPA resin is reported in this paper. The DABPA component is fluorescent in solution and in a neat state whereas the BMI component does not show any appreciable fluorescence. The BMI component quenches DABPA fluorescence and the Stern−Volmer quenching constant for this pair is reported. Fluorescence peak shapes and positions of the model succinimides have a concentration dependence. These dependencies are explained in terms of charge-transfer interactions. The results obtained in this research indicate that fluorescence signals from phenolic-like structure occur in shorter wavelength regions than those arising from phenyl succinimide moieties. Relative quantum yield measurements show DABPA to have a higher quantum efficiency than the model imides. On the basis of the fluorescence characteristics of DABPA and the imide model compounds, it should be possible to observe distinct signals for phenolic-like structure and structures containing phenylsuccinimide moieties during the cure of BMI/DABPA resin.

Model reactions involving styrene and *N*-phenylmaleimide result in the formation of a Diels−Alder−Ene adduct, or alternating copolymer or a mixture of the two depending on the reaction conditions. These results indicate that Diels−Alder−Ene and alternating copolymerization reaction sequences are both possible during the curing of BMI/DABPA.

Acknowledgment. We acknowledge the financial support in part by the National Science Foundation, Polymer Program (Grant Nos. DMR 91-08060 and 94-15385), the Army Research Office (Contract No. DAAL03-92-G-0267), and the Office of Naval Research.

References and Notes

(1) King, J. J.; Chaudari, M. A.; Zahir, S. *Int. SAMPE Symp. Exhib.* **1984**, 392.
(2) Chaudari, M. A.; Galvin, T; King, J. *Int. SAMPE Symp. Exhib.* **1985**, 735.
(3) Zahir, S.; Chaudari, M. A.; King, J. J. *Makromol. Chem., Macromol. Symp.* **1989**, *25*, 141.
(4) Carduner, K. R.; Chattha, M. S. *ACS Symp. Ser.* **1987**, *367*, 379.
(5) Abraham, T. *J. Polym. Sci. Part C: Polym. Lett.* **1988**, *26*, 521.
(6) Galvin, T.; Chaudari, M. A.; King, J. J. *Chem. Eng. Prog.* **1985**, *81* (1), 45.
(7) Barton, J. M., Hamerton, I.; Jones, J. R.; Stedman, J. C. *Polym. Bull.* **1991**, *27*, 163.
(8) *Polyimides*; Wilson, D., Stezenberger, H. D., Hergenrother, P. M., Eds.; Chapman and Hall: New York, 1990.
(9) Bell, V. L.; Young, P. R. *J. Polym. Sci., Chem. Ed.* **1986**, *24*, 2647.
(10) (a) Hedaya, J. E.; Hinman, R.; Theodoropalos, S. *J. Org. Chem.* **1966**, *31*, 1311. (b) DiGuilio, C.; Gauthier, M.; Jasse, B. *J. Appl. Polym. Sci.* **1984**, *28*, 1771.
(11) Lind, A. C.; Fry, C. G. *Polym. Mater. Sci. Eng.* **1988**, *59*, 460.
(12) Tungare, A. V.; Martin, G. C. *J. Appl. Polym. Sci.* **1992**, *46*, 1125.
(13) Sung, C. S. P.; Pyun, E.; Sun, H. L. *Macromolecules* **1986**, *19*, 2922.
(14) Kailani, M. H.; Sung, C. S. P.; Huang, S. J. *Macromolecules* **1992**, *25*, 3751.
(15) Dickinson, P. R.; Sung, C. S. P. *Macromolecules* **1992**, *25*, 3758.
(16) Song, J. C..; Sung, C. S. P. *Macromolecules* **1993**, *26*, 4818.
(17) Kim, Y. S.; Sung, C. S. P. *J. Appl. Polym. Sci.* **1995**, *57*, 363.
(18) Phelan, J. C.; Sung, C. S. P. *Polym. Mater. Sci. Eng.* **1994**, *71*, 425.
(19) Charduner, K. R.; Chattha, M. S. *ACS Polym. Mater. Sci. Eng.* **1987**, *56*, 660.
(20) (a) Stezenberger, H. D.; Koenig, P. Herzog, M.; Romer, W.; Pierce, S.; Fear, K.; Canning, M. S. *Int. SAMPE Tech Conf.* **1987**, *19*, 372. (b) Chattha, M. S.; Dickie, R. A. *J. Appl. Polym. Sci.* **1990**, *40*, 411.
(21) Mijovic, J.; Andjelic, S. *Macromolecules* **1996**, *29*, 239.
(22) (a) Cremlyn, R; Swinbourne, F; Nunes, R. *Phosphorus Sulfur* **1987**, *33*, 65. (b) Brown, A. D., Jr.; Reich, H. *J. Org. Chem.* **1970**, *35*, 1191.
(23) (a) Hall, H. K., Jr.; Nogues, P.; Rhoades, J. W.; Sentman, R. C.; Detar, M. *J. Org. Chem.* **1982**, *47*, 1451. (b) Wagner-Jauregg, Th. *Tetrahedron Lett.* **1967**, 1175.
(24) (a) Barrales-Rienda, J. M.; Gonzalez de la Campa, J. I. *J. Macromol. Sci. Chem. AII* (*2*), **1977**, 267. (b) Mohamed, A.; Jebrael, F.; El Sabee, M.; *Macromolecules* **1986**, *19*, 32.
(25) Wachsman, E. D.; Frank, C. W. *Polymer* **1988**, *29*, 1191.
(26) Hasegawa, M. Kochi, M.; Mita, I.; Yokota, R. *Eur. Polym. J.* **1989**, *25*, 349.
(27) Kotov, B. V. *Russ. J. Phys. Chem.* (*Engl. Transl.*) **1988**, *62*, 1408.
(28) Ishida, H.; Wellinghoff, S. T.; Baer, E.; Koenig, J. L. *Macromolecules* **1980**, *13*, 826.
(29) Viallat, A.; Bom, R. P.; Cohen-Addad, J. P. *Polymer* **1994**, *35*, 2731.
(30) (a) Doub, L.; Vanderbelt, J. M. *J. Am. Chem. Soc.* **1947**, *69*, 2714; **1949**, *71*, 2414. (b) Lakowicz, J. R. *Principles of Fluorescence Spectroscopy,* Plenum Press: New York, 1983.
(31) (a) Ware, W. R.; Watt, D.; Holmes, J. D. *J. Am. Chem. Soc.* **1974**, *96*, 7853. (b) Taylor, G. N. *Chem. Phys. Lett.* **1971**, *10*, 355. (c) Ware, W. R.; Holmes, J. D.; Arnold, D. R. *J. Am. Chem. Soc.* **1974**, *96*, 7861. (d) Ware, W. R.; O'Conner, D. V. *J. Am. Chem. Soc.* **1974**, *98*, 4706. (e) Ware, W. R.; Watt, D.; Hui, M. H. *J. Am. Chem. Soc.* **1974**, *98*, 4712.
(32) *Luminescence Techniques in Solid State Polymer Research;* Zlatkevich, L., Ed., Marcel Dekker, Inc.: New York, 1989.
(33) So, Y.; Zaleski, J.; Merlick, C.; Ellaboudy, A. *Macromolecules* **1996**, *29*, 2783.

MA9618888